PCCP

PAPER

View Article Online
View Journal | View Issue

Cite this: *Phys. Chem. Chem. Phys.*, 2016, **18**, 14449

Thickness dependence of surface energy and contact angle of water droplets on ultrathin MoS_2 films†

Yanhua Guo,[ab] Zhengfei Wang,[b] Lizhi Zhang,[b] Xiaodong Shen[a] and Feng Liu*[b]

Received 4th January 2016,
Accepted 29th April 2016

DOI: 10.1039/c6cp00036c

www.rsc.org/pccp

We have performed a systematic density functional study of surface energy of MoS_2 films as a function of thickness from one to twelve layers with the consideration of van der Waals (vdW) interactions using the vdW-DF and DFT-D2 methods. Both vdW schemes show that the surface energy will increase with the increase of the number of atomic layers and converge to a constant value at about six layers. Based on the calculated surface energies, we further analyze the surface contact angle of water droplets on the MoS_2 film surface using Young's equation as a function of thickness in comparison with experiments, from which the water–MoS_2 interfacial energy is derived to be independent of MoS_2 thickness. Our calculations indicate that the vdW interactions between the MoS_2 layers play an important role in determining surface energy, and results in the thickness dependence of the contact angle of water droplets on the MoS_2 film surface. Our results explain well the recent wetting experiment [*Nano Lett.*, 2014, **14**(8), 4314], and will be useful for future studies of physical and chemical properties of ultrathin MoS_2 films.

1. Introduction

The successful exfoliation of single-layer graphene[1,2] has opened up new possibilities for the investigation of two-dimensional (2D) materials.[3–10] Extensive studies have shown that 2D materials exhibit unique and distinctive properties different from their 3D counterparts. For instance, the linear band dispersion gives rise to an anomalous quantum Hall effect in single-layer graphene at room temperature, resulting in a new category of "Fermi–Dirac" materials.[2] Besides graphene, one of the most well-studied 2D materials is the layered transition metal dichalcogenides (TMDCs), such as MoS_2. It is built up of van der Waals (vdW) bonded layers which consist of an atomic plane of Mo atoms sandwiched between two atomic planes of S atoms. The weak interlayer interaction allows for their exfoliation down to single- and a few-layer forms through micromechanical cleavage[11] or liquid phase exfoliation.[12] In contrast to gapless graphene, single-layer MoS_2 has a direct bandgap in addition to moderately high field-effect mobilities[13,14] and efficient light emission, which make it a promising candidate for low-power digital electronics[15] and optoelectronics applications.[16]

Recent studies have established the influence of the number of layers and stacking orders on the electronic and optical properties of TMDCs.[17–21] Mak *et al.*[11] found that the bandgap increases (1.3 eV to 1.8 eV) and transforms from indirect to direct when MoS_2 is thinned to atomically thin sheets from the bulk, and showed that this bandgap transition is due to quantum confinement in the *c*-axis of the crystal. The direct bandgap results in photoluminescence from monolayer MoS_2,[20] and also enables valley polarization which is not seen in bilayer MoS_2.[22] Additionally, there is an obvious change in the photoconductivity spectra, absorption, and electrocatalysis of ultrathin film MoS_2, which in general represents a strong thickness dependence. Similar to MoS_2, the layer-dependent electronic structure of WSe_2 has been reported by Yeh *et al.*[23] lately, exhibiting a shift of the valence-band maximum from $\bar{\Gamma}$ (multilayer WSe_2) to $\bar{K}$ (single-layer WSe_2).

Since a 2D material is entirely made up of its surface, it is extremely important to understand its surface properties for the use of coatings, microfluidic applications and performance of nanoelectronic devices. It has been well recognized that many surface properties are related to surface energy, which is the most fundamental parameter that characterizes the surface and its interaction with other materials. However, surface energy is difficult to measure directly *via* experiment. The methods used most frequently for surface free energy determination rely on wetting contact angle measurements. Several theories and approaches have been proposed to derive surface free energy of a solid surface using the contact angle information. It is noted that the values of surface energy are different depending on different

[a] *College of Materials Science and Engineering, Nanjing Tech University, Nanjing, 210009, China*
[b] *Department of Materials Science and Engineering, University of Utah, Utah 84112, USA. E-mail: fliu@eng.utah.edu*

† Electronic supplementary information (ESI) available. See DOI: 10.1039/c6cp00036c

surface energy models, even if the same contact angle data are used.[24] Specifically, for MoS_2 thin films, Gaur *et al.*[8] have recently reported a layer thickness dependence of its wettability *via* static contact angle measurements. It shows that the 11-layer MoS_2 film has a similar wetting behavior to the single crystal, while the contact angle decreases from 98° to 94° for mono- and bilayer MoS_2 films.

In this paper, we perform a comprehensive theoretical study of surface energy of MoS_2 ultrathin films by virtue of first-principles supercell slab calculations based on density functional theory. The evolutions of surface energy of multi-layers of MoS_2 with increasing number of layers (n = 1 to 12) are investigated *via* two approaches (vdW-DF and DFT-D2), accounting for the vdW interactions. Also, two different stacking layer sequences are considered. Based on the calculated surface energies, we further analyze the surface contact angle of water droplets on the MoS_2 film surface using Young's equation as a function of thickness in comparison with experiments. It reveals that the water–MoS_2 interfacial energy is independent of film thickness.

2. Computational method

Our density functional theory (DFT) calculations employ the Vienna *ab initio* Simulation Package,[25] equipped with the projector augmented wave method[26] for electron–ion interactions. The generalized gradient approximation in the form of the PBE-type parameterization is implemented for the exchange interaction of electrons. The electronic wave functions have been expanded in a plane-wave basis with an energy cutoff of 600 eV. The Brillouin zone was sampled by 12 × 12 × 1 special mesh points in k space based on the Monkhorst–Pack scheme. Atomic positions and lattice parameters in all structures are measured by employing the conjugate-gradient algorithm. The self-consistency was achieved with a tolerance when the total energy difference between the last two consecutive steps is less than 10^{-6} eV and the maximum Hellmann–Feynman force on each atom is less than 10^{-2} eV Å^{-1}.

All surface calculations were performed using the slab technique, implemented using the periodically repeating infinite layers separated by vacuum layers along the surface normal. A vacuum thickness of 30 Å is adopted in all cases in order to remove interaction between the slab layers. We assess two long-range vdW correction methods due to the fact that standard DFT calculations are unable to describe vdW interactions accurately as shown extensively in the literature. The first is the DFT-D2 approach of Grimme,[27] which adds a semiempirical pairwise force field to the conventional Kohn–Sham DFT energy. The second is the vdW-DF approach proposed by Dion *et al.*,[28] which includes a nonlocal vdW correlation functional added to the exchange–correlation energy.

3. Results and discussion

The 3D bulk MoS_2 has three different polytypes, 1T, 2H, and 3R, wherein the S atoms are octahedrally coordinated in the 1T structure, in contrast to the prismatic coordination of S in the 2H and 3R phases. Because the 1T phase of one molecular layer is found to be unstable,[29] we considered the 2H and 3R phases to obtain the lattice parameters of MoS_2 films. Although the 3R-MoS_2 is usually reported to be a high pressure polytype, recent experimental and theoretical studies point out the existence of the 3R phase in low dimensional materials[30] due to inherent strain. Both 2H and 3R MoS_2 polytypes are built up from layers consisting of an atomic plane of Mo sandwiched between two atomic S planes having the same 2D hexagonal lattice in a trigonal prismatic arrangement. The only difference between the two phases is the layer stacking sequence. The MoS_2 layers are arranged in antiparallel AB stacking sequence in 2H-MoS_2, but parallel ABC in the 3R phase. As a benchmark, the structural properties of bulk MoS_2 are calculated at first (see the ESI†), showing good agreement with previous theoretical studies.[31,32] In comparison with the experiments, the DFT-D2 method shows much better values of the lattice parameter parallel to the stacking direction, while the vdW-DF theory tends to systematically overestimate these values. And our calculations show similar stability of the two phases.

Based on the optimized lattice parameters of bulk structures, we consider two types of multilayers of MoS_2 with different stacking configurations. Fig. 1 shows these two stacking sequences of AB (Fig. 1(a)) and ABC configurations (Fig. 1(b)). In the AB stacking, S atoms in the first layer are located above Mo atoms of the second layer, resulting in a slight shift along the a-axis while the third layer S atoms will be in the same atomic positions as the first layer. The difference in the ABC stacking is that only the fourth layer will have the same atomic positions as the first one. We have optimized the multi-layered MoS_2 structures of the two different stackings from monolayer (n = 1) to twelve layers (n = 12).

Next, we evaluated the surface energies of the MoS_2 films as a function of the number of layers (n) ranging from 1 to 12. The surface energy of an n-layer slab is given by the following expression:

$$E_{\mathrm{surf}}(n) = \frac{1}{2S}(E_{\mathrm{n}} - NE_{\mathrm{b}}) \quad (1)$$

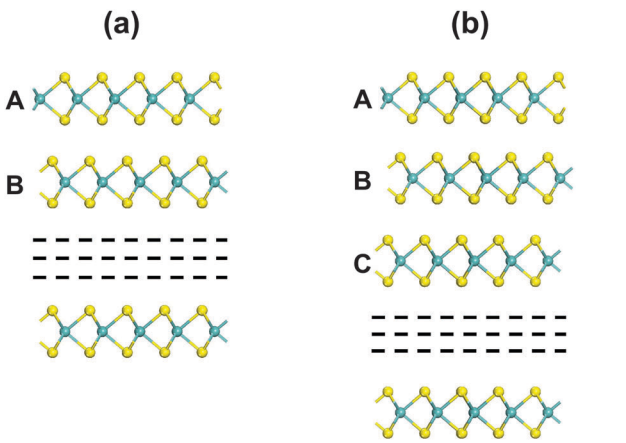

Fig. 1 The optimized geometric structures of n-layered MoS_2 with two stacking configurations: (a) AB and (b) ABC. Side view of the 3 × 3 super-cell. Yellow and blue spheres represent S and Mo atoms, respectively.

where E_n is the total slab energy per primitive surface unit cell, N is the number of atoms in the slab, and S is the surface cell area. The choice of E_b, which represents the total energy per primitive bulk unit cell, is quite crucial in our calculation. In the conventional method, the bulk atom energy E_b is in general obtained from a separate calculation of the corresponding bulk, *i.e.*, from the 2H and 3R phase MoS_2 bulk in our calculations. However, the surface energies obtained in this way keep decreasing with the increase in thickness without convergence. It is caused by systematic errors due to the different accuracies in the slab and bulk calculations.[33,34] Herein, we obtain the bulk atom energy E_b by using the 'slab method' to ensure the convergence of the surface energy with increasing layers. Eqn (1) indicates a linear relationship between the total slab energy E_n and the number of atoms (N) in the slab as the surface energy E_{surf} becomes constant when N is sufficiently large. Therefore, the slope of the linear E_n–N curve at large N gives an accurate measure of the bulk atom energy.

The calculated surface energy curves from the DFT-D2 and vdW-DF calculations are shown in Fig. 2 as a function of layer thickness. As one can see, for the two types of stackings (AB and ABC), there is a good agreement of the surface energies obtained by the same method, which indicates the similar stability for all the configurations. For different methods, the variations of the surface energy with the increasing number of layers are predicted to be similar. Fig. 2 shows that the surface energies are very sensitive to the thickness of ultrathin MoS_2 films, increasing smoothly with an increase in the number of layers. When the slab thickness, n, reaches about six layers, the surface energies are well converged, which implies that the slabs with more than seven atomic layers possess a bulk-like interior. Especially in the DFT-D2 approach, the total energy of the system is defined as a sum of the self-consistent Kohn–Sham energy and a semiempirical correction:

$$E_{DFT\text{-}D} = E_{KS\text{-}DFT} + E_{disp} \quad (2)$$

E_{disp} represents the vdW interactions which have been computed using the semiempirical correction of Grimme. We show the evolution of E_{disp} as a function of number of layers in Fig. 3.

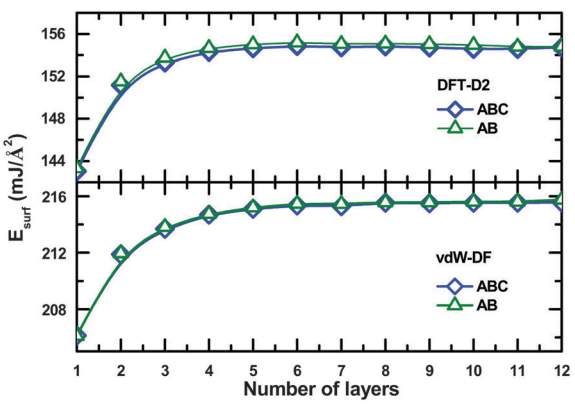

Fig. 2 Surface energy as a function of number of atomic layers for MoS_2 with two stacking configurations: AB in DFT-D2 (uptriangle), AB in vdW-DF (downtriangle), ABC in DFT-D2 (circle) and ABC in vdW-DF (square).

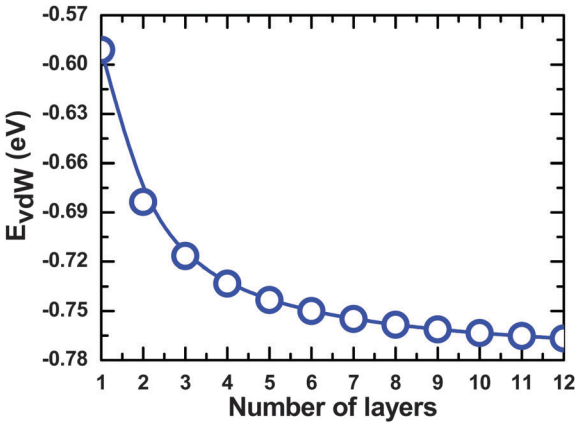

Fig. 3 Evolutions of van der Waals interactions as a function of the number of MoS_2 layers obtained using the DFT-D2 method.

The values of E_{disp} decrease with the increasing number of layers, indicating increasing vdW interactions. Similar to surface energy, when the number of layers n becomes big enough ($\sim$6 layers), the vdW interactions become constant. Therefore, the strong thickness dependence of vdW interactions gives rise to a strong thickness dependence of surface energy.

Now we analyze the dependence of the wettability of MoS_2 on layer thickness, and derive the water–MoS_2 interfacial energy as a function of number of layers by comparing our theory with the experiments.[8] The contact angle is given by the Young's equation as:[35]

$$\cos\theta = \frac{\gamma_s - \gamma_{sl}}{\gamma_l} \quad (3)$$

where γ_s, γ_l, and γ_{sl} represent the solid surface free energy, liquid surface free energy, and solid–liquid interfacial energy, respectively. Here, we choose the surface free energy of water (γ_l) as 72 mJ m^{-2}.[8] Eqn (3) shows that quantitatively, the values of $\cos\theta$ will increase with an increase of γ_s in the case of a constant value of γ_{sl}, which means that θ will decrease. Indeed, based on our calculated surface energies as shown in Fig. 2, θ should decrease with the increasing layer thickness, consistent with the experiments.[8] Furthermore, we can derive the water–MoS_2 interfacial energy by combining the experimental results and our calculations. Gaur *et al.*[8] have measured the contact angles with water for monolayer (97.83°), bilayer (94.37°) and 11-layer (88.37°) MoS_2, and confirmed a similar wetting behavior for bulk and MoS_2 films with 11 layers. Thus, we are able to obtain the interfacial energies between H_2O and the n-layer MoS_2 film (n = 1, 2, 11) respectively from eqn (3). The derived values of γ_{sl} are calculated to be 152.85, 156.66 and 152.64 mJ m^{-2} using the DFT-D2 method, and 215.94, 217.37 and 213.49 mJ m^{-2} using the vdW-DF method, respectively. The two methods show that the variations of γ_{sl} are only $\sim$2–3%, well within the theoretical and experimental error bars. Therefore, our analysis indicates that the water–MoS_2 interfacial energy is insensitive to the thickness of the MoS_2 film. Taking the average value of water–MoS_2 interfacial energy γ_{sl} = 154.05 mJ m^{-2} (DFT-D2) or 215.6 mJ m^{-2} (vdW-DF), the contact angles of water droplets

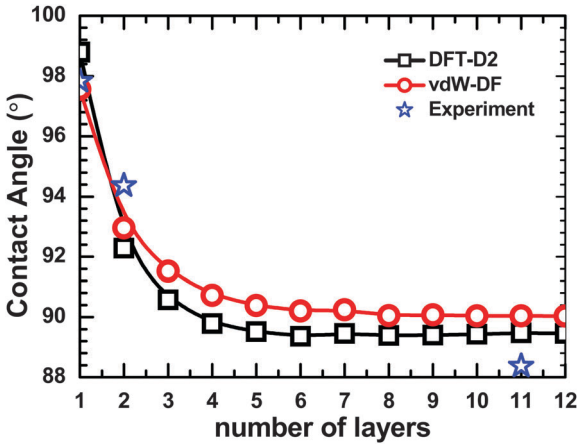

Fig. 4 Evolution of contact angle with the layer number of MoS_2 using different calculation theories (DFT-D2 *vs.* vdW-DF).

on the MoS_2 film surface as a function of thickness can be determined *via* eqn (3), and the results are shown in Fig. 4. The contact angle exhibits strong thickness dependence, especially for the ultrathin MoS_2 film, due prominently to the changing surface energy. When the number of MoS_2 layers goes beyond six, the contact angle becomes almost unchanged. The enhanced long-range vdW forces which are responsible for the modification of surface energy will in turn induce reduction of contact angle of H_2O on the MoS_2 film.

4. Conclusion

In conclusion, we have performed a quantitative analysis of surface energy and the contact angle of water droplets on MoS_2 films as a function of thickness. We show that there is a very strong thickness dependence of surface energy and hence the contact angle, due to the changing vdW interlayer interactions in ultrathin films of less than six layers. The converged surface energy at a thicker film is calculated to be 154.58 mJ m^{-2} (DFT-D2) and 215.55 mJ m^{-2} (vdW-DF) for both AB and ABC stacking sequences, while the water–MoS_2 interfacial energy is independent of thickness. Our results explain the recent water wetting experiments of MoS_2 films, and provide important thermodynamic surface/interface data for future studies of MoS_2 films as well as their applications.

Acknowledgements

Z. Wang and F. Liu thank the financial support from DOE-BES (Grant No. DE-FG02-04ER46148). Yanhua Guo acknowledges China Scholarship Council (Grant No. 201408320015). We thank the CHPC at the University of Utah and DOE-NERSC for providing the computing resources.

References

1 K. S. Novoselov, D. Jiang, F. Schedin, T. J. Booth, V. V. Khotkevich, S. V. Morozov and A. K. Geim, *Proc. Natl. Acad. Sci. U. S. A.*, 2005, **102**, 10451.
2 K. S. Novoselov, Z. Jiang, Y. Zhang, S. V. Morozov, H. L. Stormer, U. Zeitler, J. C. Maan, G. S. Boebinger, P. Kim and A. K. Geim, *Science*, 2007, **315**, 1379.
3 L. K. Li, Y. J. Yu, G. J. Ye, Q. Q. Ge, X. D. Ou, H. Wu, D. L. Feng, X. H. Chen and Y. B. Zhang, *Nat. Nanotechnol.*, 2014, **9**, 372.
4 Z. F. Wang, Z. Liu and F. Liu, *Phys. Rev. Lett.*, 2013, **110**, 196801.
5 Z. Liu, Z. F. Wang, J. W. Mei, Y. S. Wu and F. Liu, *Phys. Rev. Lett.*, 2013, **110**, 106804.
6 Z. F. Wang, Z. Liu and F. Liu, *Nat. Commun.*, 2013, **4**, 1471.
7 Z. F. Wang, N. H. Su and F. Liu, *Nano Lett.*, 2013, **13**, 2842.
8 A. P. S. Gaur, S. Sahoo, M. Ahmadi, S. P. Dash, M. J.-F. Guinel and R. S. Katiyar, *Nano Lett.*, 2014, **14**, 4314.
9 A. H. CastroNeto, *Phys. Rev. Lett.*, 2001, **86**, 4382.
10 K. Rossnagel, *J. Phys.: Condens. Matter*, 2011, **23**, 213001.
11 K. F. Mak, C. Lee, J. Hone, J. Shan and T. F. Heinz, *Phys. Rev. Lett.*, 2010, **105**, 136805.
12 R. J. Smith, P. J. King, M. Lotya, C. Wirtz, U. Khan, S. De, A. O'Neill, G. S. Duesberg, J. C. Grunlan, G. Moriarty, J. Chen, J. Z. Wang, A. I. Minett, V. Nicolosi and J. N. Coleman, *Adv. Mater.*, 2011, **23**, 3944.
13 W. Bao, X. Cai, D. Kim, K. Sridhara and M. S. Fuhrer, *Appl. Phys. Lett.*, 2013, **102**, 042104.
14 N. Pradhan, D. Rhodes, Q. Zhang, S. Talapatra, M. Terrones, P. Ajayan and L. Balicas, *Appl. Phys. Lett.*, 2013, **102**, 123105.
15 Y. Zhang, J. Ye, Y. Matsuhashi and Y. Iwasa, *Nano Lett.*, 2012, **12**, 1136.
16 W. Choi, M. Y. Cho, A. Konar, J. H. Lee, G. B. Cha, S. C. Hong, S. Kim, J. Kim, D. Jena and J. Joo, *Adv. Mater.*, 2012, **24**, 5832.
17 S.-L. Li, H. Miyazaki, H. S. Song, H. Kuramochi, S. Nakaharai and K. Tsukagoshi, *ACS Nano*, 2012, **6**(8), 7381.
18 S.-L. Li, K. Wakabayashi, Y. Xu, S. Nakaharai, K. Komatsu, W.-W. Li, Y.-F. Lin, A. Aparecido-Ferreira and K. Tsukagoshi, *Nano Lett.*, 2013, **13**(8), 3546.
19 S.-L. Li, K. Katsuyoshi, S. Nakaharai, Y.-F. Lin, M. Yamamoto, X. F. Duan and K. Tsukagoshi, *ACS Nano*, 2014, **8**(12), 12836.
20 A. Splendiani, L. Sun, Y. B. Zhang, T. S. Li, J. Kim, C.-Y. Chim, G. Galli and F. Wang, *Nano Lett.*, 2010, **10**, 1271.
21 H. S. Lee, S.-W. Min, Y.-G. Chang, M. K. Park, T. Nam, H. Kim, J. H. Kim, S. Ryu and S. Im, *Nano Lett.*, 2012, **12**, 3695.
22 K. F. Mak, K. He, J. Shan and T. F. Heinz, *Nat. Nanotechnol.*, 2012, **7**, 494.
23 P.-C. Yeh, W. Jin, N. Zaki, D. Zhang, J. T. Liou, J. T. Sadowski, A. Al-Mahboob, J. I. Dadap, I. P. Herman, P. Sutter and R. M. Osgood, *Phys. Rev. B: Condens. Matter Mater. Phys.*, 2015, **91**, 041407(R).
24 A. Kozbial, Z. T. Li, C. Conaway, R. McGinley, S. Dhingra, V. Vahdat, F. Zhou, B. D'Urso, H. T. Liu and L. Li, *Langmuir*, 2014, **30**, 8598.
25 G. Kresse and J. Furthmüller, *Phys. Rev. B: Condens. Matter Mater. Phys.*, 1996, **54**, 11169.
26 G. Kresse and D. Joubert, *Phys. Rev. B: Condens. Matter Mater. Phys.*, 1999, **59**, 1758.

27 T. Bučko, J. Hafner, S. Lebègue and J. G. Ángyán, *J. Phys. Chem. A*, 2010, **114**, 11814.
28 H. Rydberg, B. I. Lundqvist, D. C. Langreth and M. Dion, *Phys. Rev. B: Condens. Matter Mater. Phys.*, 2000, **62**, 6997.
29 ed. W. Müller-Warmuth and R. Schöllhorn, *Progress in Intercalation Research*, Springer, New York, 1994, vol. 17, p. 50.
30 L. Houben, A. N. Enyashin, Y. Feldman, R. Rosentsveig, D. G. Stroppa and M. Bar-Sadan, *J. Phys. Chem. C*, 2012, **116**, 24350.
31 H. Rydberg, M. Dion, N. Jacobson, E. Schröder, P. Hyldgaard, S. I. Simak, D. C. Langreth and B. I. Lundqvist, *Phys. Rev. Lett.*, 2003, **91**, 126402.
32 M. Mortazavi, C. Wang, J. K. Deng, V. B. Shenoy and N. V. Medhekar, *J. Power Sources*, 2014, **268**, 279.
33 V. Fiorentini and M. Methfessel, *J. Phys.: Condens. Matter*, 1996, **8**, 6525.
34 G. H. Lu, M. H. Huang, M. Cuma and F. Liu, *Surf. Sci.*, 2005, **588**, 61.
35 F. Liu, *Phys. Rev. Lett.*, 2002, **89**, 246105.